Exergy Analysis of a Ground-Source Heat Pump System

Kathrin Menberg[1,2], Yeonsook Heo[2], Wonjun Choi[3], Ryozo Ooka[3], Ruchi Choudhary[1], Masanori Shukuya[4]

[1] University of Cambridge, Department of Engineering, Cambridge, UK,
[2] University of Cambridge, Department of Architecture, Cambridge, UK,
[3] University of Tokyo, Institute of Industrial Science, Tokyo, Japan,
[4] Tokyo City University, Department of Restoration Ecology and Built Environment, Tokyo, Japan

Abstract

In contrast to energy analysis, the analysis of exergy allows the evaluation of the *quality* of different energy flows and enables a comprehensive assessment of the performance of a system and its individual components by accounting for necessary exergy consumption and unnecessary consumption. While exergy analysis methods have been applied to a variety of conventional and renewable energy supply systems, there is still a lack of knowledge regarding the detailed exergy flows and exergy efficiencies of ground-source heat pump systems (GSHP).

In this study, we develop a thermodynamic model for a ground-sourced cooling system of an existing building by applying the concept of cool and warm exergy. In addition, we investigate the effect of varying temperature conditions, such as reference and ground temperatures, on the exergy flows and system performance.

Introduction

In thermodynamics, the exergy content of a system is defined as the maximum theoretical amount of work that can be extracted from the system in relation to a certain reference state. The analysis of exergy contents and flows offers a concept to assess the quality of energy, which has hitherto been applied in various fields of engineering and science (Li et al., 2014).

Energy analysis methods, which are based on the principle of energy conservation, are often inadequate for gaining a full understanding of all important aspects of energy utilisation in energy supply systems (Schmidt, 2009). The analysis of exergy on the other hand allows evaluation of the quality of energy flows through individual components of an energy supply system and thus enables a localised assessment of subsystem efficiencies. As a result, the magnitude and location of thermodynamic inefficiencies can be pinpointed and options for system improvement can be identified.

The large potential of exergy analysis with regard to performance evaluation has led to an increasing number of studies applying these methods to a large variety of energy supply systems. However, most of these studies regard exergy consumption of lumped subsystem components, such as the distribution system, heating system or the building envelope (Schmidt, 2009; Kazanci, 2016). So far, few studies have evaluated the exergy performance of the different components of a GSHP system in detail (Li et al., 2014). While some studies evaluated the effect of varying reference, i.e. outdoor, conditions on the overall exergy performance of an energy supply system (Zhou & Gong, 2013), there is still a lack of knowledge regarding sub-system components. In addition, a detailed thermodynamic model consisting of a number of sub-system components often operates under various temperature boundary conditions, such as ground and indoor temperature, which might have very diverse effects on the exergy performance.

In this study, we analyse the exergy performance of a GSHP system with a radiant ceiling. We do so by applying the concept of warm and cool exergy to the thermodynamic model of the system. The model includes formulations for the energy and exergy terms for all individual subsystems, such as the heat pump, mixing valve and the radiant ceiling, which allows an in-depth analysis of the exergy flows and consumption for each subsystem. As tools for exergy analysis of energy systems are currently not incorporated in common building simulation packages, such as TRNSYS or EnergyPlus, the formulation of our model also comprises a first step towards introducing exergy analysis to the transient building simulation framework and adds to the promotion of exergy analyses within existing energy simulation tools.

In addition, we assess the effect that variations in the boundary conditions, such as reference and ground temperature, and internal system temperatures (such as the temperature difference between inlet and outlet flow), have on the system's exergy performance. Typically, exergy analysis is carried out for one set of temperature conditions including internal system temperatures and the reference temperature, which is assumed representative for the system's environment and period of interest (Figure 1).

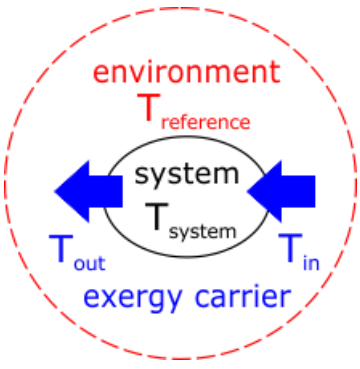

Figure 1: Key temperature terms of an exergy model.

As energy supply systems provide indoor heating and cooling with respect to the outdoor conditions, the outdoor ambient air temperature is the most obvious choice for the reference temperature. Accordingly, all exergy contents or consumptions are quantified with respect to the outdoor thermal state, which will directly influence the magnitude of the exergy values. The individual impact of the reference and system temperatures on exergy output and consumption are evaluated per component by assigning parametric temperature changes. To quantify the magnitude of the overall effect and identify those temperature parameters that have the most significant influence on the overall exergy performance, we conduct a sensitivity analysis using Morris method.

Methodology

Exergy analysis

According to Shukuya (2013) exergy is defined as a measure for the dispersion potential of energy, while entropy is a measure for this dispersion of energy. Furthermore, exergy can be considered as warm or cool exergy, depending on the system temperature T and the reference temperature T_0. If the system temperature T is higher than T_0, the thermal energy Q contained in the system can disperse into the environment, which acts as a cold reservoir, as a flow of warm exergy (eq. 1). If the environment is warmer than the system, exergy in form of cool exergy can flow out of the system into the environment, denoting the lack of thermal energy by *(-Q*)* (eq. 2) (Shukuya, 2013).

$$X_{warm} = (1 - \frac{T_0}{T})\, Q, for\ T > T_0 \quad (1)$$

$$X_{cool} = (1 - \frac{T_0}{T})\, (-Q^*), for\ T_0 > T \quad (2)$$

For any system under consideration, one can obtain the general energy balance equation according to the principle of energy conservation.

$$[energy\ input] = [energy\ stored] + [energy\ output] \quad (3)$$

Furthermore, because of the relation of energy and entropy (eq. 4a), a general exergy balance equation for any system can be written as eq. 4b (Li et al., 2014).

$$exergy = energy - entropy \cdot T_0 \quad (4a)$$

$$[exergy\ input] - [exergy\ consumed] = [exergy\ stored] + [exergy\ output] \quad (4b)$$

These equations state that the exergy inputs into any system or component, such as the exergy contained in fluids that enter the system, minus the exergy consumed during heat transfer in that system, are equal to the sum of exergy outputs, such as cool exergy delivered to a room or exergy contained in outlet flow.

System overview

The GSHP system used as a case study for the exergy analysis is installed in the Architecture Studio Building at the University of Cambridge and supplies cooling for a large open office space. It consists of two vertical borehole heat exchangers (BHEs) and a reversible brine-to-water heat pump (HP). Thermal energy is supplied to (or extracted from) the room by radiant ceiling panels.

In order to analyse the exergy flow through the energy supply system and the exergy consumption in the individual components, it is necessary to divide the system into its basic components (Li et al., 2014). For the hybrid system operating in cooling mode, these include: the borehole heat exchanger, the condenser of the heat pump, the refrigerant in the heat pump cycle, the evaporator of the heat pump, the mixing valve after the heat pump and the radiant ceiling (Figure 2).

The BHE is used to cool down the heat carrier fluid in the BHE, which enters the condenser side of the heat pump, where the compressed, but still vapour-state refrigerant fluid condenses and releases heat into the BHE loop fluid. In the expansion valve, a distinct pressure drop leads to the evaporation of the liquid refrigerant, which then enters the evaporator side of the heat pump at a low temperature and by receiving heat from the load side fluid cools the medium circulating through the radiant ceiling panels flow. The main return flow from the ceiling panels in the building is split before the heat pump, so that only a fraction of the main circulation flow passes through the evaporator of the heat pump. The other fraction of the flow bypasses the heat pump, and both flows are then brought together in the heat pump mixing valve, which represents the supply flow to the ceiling panels.

Modelling Approach

In the following paragraphs, the energy and exergy equations are specified for each component following the general approach of Li et al. (2014), based on the concept of warm and cool exergy. If not stated otherwise, temperatures are given in Kelvin, exergy values in kW and exergy efficiency values in percent.

Borehole heat exchanger

Based on the energy and exergy balance equations (eqs. 3 and 4), corresponding equations can be defined for the heat carrier fluid in the BHE and the ground (eqs. 5 and 6).

$$c_b m_b (T_{w,re} - T_0) + (-Q_g) = c_b m_b (T_w - T_0) \quad (5)$$

$$X_{w,re} + X_g - X_{gex} = X_w \quad (6)$$

In eq. 5, the energy exchanged with the ground Q_g, which is typically defined to be positive for the flow direction into the heat carrier fluid from the ground, is assigned a negative sign as it is directed towards the ground. The terms $c_b m_b (T_{w,re} - T_0)$ and $c_b m_b (T_w - T_0)$ quantify the amount of thermal energy contained in the BHE outlet and inlet flow, respectively, specified by the mass flow rate m_b and the corresponding temperatures (Table 1). The heat carrier mass flow rate in the BHE, m_b, was set to 0.6 kg/s with a heat capacity c_b of 4.27 kJ/(kg K) according to the system's design specifications.

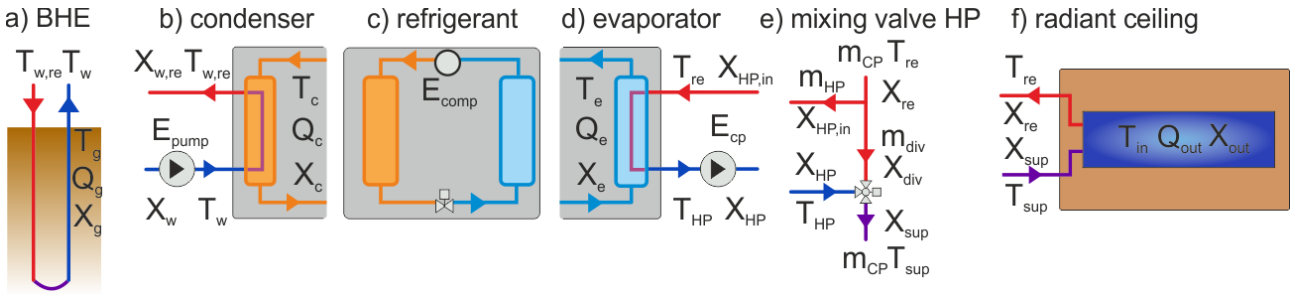

Figure 2: Individual components of the GSHP system with the energy, exergy and temperature terms applying to the corresponding components.

In eq. 6, the exergy extracted from the ground X_g comprises cool exergy, as the internal sub-system temperature T_g is lower than the reference temperature T_0 outside of the system, and can be defined according to eq. 7. $X_{w,re}$ is the exergy of the heat carrier fluid return flow (eq. 8), while X_{gex} is the exergy consumption during heat exchange with the ground, and X_w is the output exergy comprised in the BHE outlet flow (eq. 9).

$$X_g = \left(1 - \frac{T_0}{T_g}\right)(-Q_g) \tag{7}$$

$$X_{w,re} = c_b m_b \left\{(T_{w,re} - T_0) - T_0 \, ln \frac{T_{w,re}}{T_0}\right\} \tag{8}$$

$$X_w = c_b m_b \left\{(T_w - T_0) - T_0 \, ln \frac{T_w}{T_0}\right\} \tag{9}$$

Condenser of the heat pump

The energy and exergy balances of the condenser within the heat pump are given in eqs. 10 and 11, which also consider the electricity to drive the ground loop pump E_{pump} (0.38 kW) as an energy input. Eq. 11 has two input terms, X_w and E_{pump}, as well as two output terms, $X_{w,re}$ and X_c, which represents the exergy output into the refrigerant (eq. 12). X_{cond} quantifies the exergy consumption in the condenser.

$$E_{pump} + c_b m_b (T_w - T_0) = c_b m_b (T_{w,re} - T_0) + (-Q_c) \tag{10}$$

$$E_{pump} + X_w - X_{cond} = X_{w,re} + X_c \tag{11}$$

$$X_c = \left(1 - \frac{T_0}{T_c}\right)(-Q_c) \tag{12}$$

Refrigerant cycle

The energy and exergy balance equations (eq. 13, 14) of the refrigerant loop in the heat pump can be defined based on the according input (Q_e, X_e) and output (Q_c, X_c) terms and accounting for the electricity demand of the compressor E_{comp} (1.25 kW) and the exergy consumption in the refrigerant cycle $X_{refcycle}$.

$$E_{comp} + Q_e = Q_c \tag{13}$$

$$E_{comp} + X_c - X_{refcycle} = X_e \tag{14}$$

Evaporator of the heat pump

The energy balance of the evaporator side of the heat pump in cooling mode is specified by eq. 15 and takes into account the thermal energy content of the inlet and outlet flow m_{HP} of the heat pump load side and the power consumption of the main circulation pump E_{CP} (0.63 kW). The heat capacity of the load side fluid c_w was assumed to be 4.19 kJ/(kg K). The corresponding exergy balance (eq. 16) has three input terms: E_{CP}, the exergy input from the refrigerant at the evaporator X_e (eq. 17), and the exergy content of the inlet flow $X_{HP,in}$ (eq. 18). The exergy of the load side outlet flow X_{HP} represents the exergy output of the component (eq. 19), and the exergy consumption in the evaporator is denoted by X_{evap}.

$$E_{Cp} + (-Q_e) + c_w m_{HP} (T_{re} - T_0) = c_w m_{HP} (T_{HP} - T_0) \tag{15}$$

$$E_{CP} + X_e + X_{HP,in} - X_{evap} = X_{HP} \tag{16}$$

$$X_e = \left(1 - \frac{T_0}{T_e}\right)(-Q_e) \tag{17}$$

$$X_{HP,in} = c_w m_{HP} \left\{(T_{re} - T_0) - T_0 \, ln \frac{T_{re}}{T_0}\right\} \tag{18}$$

$$X_{HP} = c_w m_{HP} \left\{(T_{HP} - T_0) - T_0 \, ln \frac{T_{HP}}{T_0}\right\} \tag{19}$$

Mixing valve after the heat pump

The energy balance for the HP mixing valve, where the flow through the HP, m_{HP}, is combined with the diverted flow that bypasses the heat pump, m_{divHP}, is defined by the contents of thermal energy of the two inlet flows and the outlet flow m_{CP} (eq. 20). The exergy balance (eq. 21) is formed of the corresponding exergy contents of the inlet, X_{HP} (eq. 19) and X_{divHP} (eq. 22), and outlet flows X_{sup} (eq. 23), and an exergy consumption term X_{valHP}, which accounts for entropy generated during the mixing process.

$$c_w m_{HP} (T_{HP} - T_0) + c_w m_{divHP} (T_{re} - T_0) = c_w m_{CP} (T_{sup} - T_0) \tag{20}$$

$$X_{divHP} + X_{HP} - X_{valHP} = X_{sup} \tag{21}$$

$$X_{divHP} = c_w m_{divHP} \left\{(T_{re} - T_0) - T_0 \, ln \frac{T_{re}}{T_0}\right\} \tag{22}$$

$$X_{sup} = c_w m_{CP} \left\{(T_{sup} - T_0) - T_0 \, ln \frac{T_{sup}}{T_0}\right\} \tag{23}$$

Radiant ceiling

The energy balance for the radiant ceiling subsystem is given by eq. 24, where T_{in} denotes the indoor room temperature, and the corresponding exergy balance by eq. 25. Exergy input is provided by the exergy of the supply flow

X_{sup} (eq. 23), while the output term is formed of the exergy content of the return flow X_{re} (eq. 27) and the exergy delivered to the room X_{out} (eq. 26). X_{ceil} denotes exergy consumption during heat exchange in the ceiling.

$$c_w m_{CP}(T_{sup} - T_{in}) = c_w m_{CP}(T_{re} - T_{in}) + (-Q_{out}) \quad (24)$$

$$X_{sup} - X_{ceil} = X_{re} + X_{out} \quad (25)$$

$$-X_{out} = \left(1 - \frac{T_0}{T_{in}}\right)(-Q_{out}) \quad (26)$$

$$X_{re} = c_w m_{CP}\left\{(T_{re} - T_0) - T_0 \ln \frac{T_{re}}{T_0}\right\} \quad (27)$$

Exergy Performance Indicators

To assess the exergy performance of the cooling system we apply three different exergy ratios. As exergy efficiency measures for the system performance, we adopt the net exergy efficiency η_1 and the natural exergy ratio of the system η_2 from Li et al. (2014). In addition, we define an additional measure for the true exergy efficiency of the system η_3:

$$\eta_1 = \frac{exergy\ output}{non-natural\ exergy\ input} = \frac{X_{out}}{E_{comp} + E_{CP} + E_{pump}} \quad (28)$$

$$\eta_2 = \frac{natural\ exergy\ input}{total\ exergy\ input} = \frac{X_g}{E_{comp} + E_{CP} + E_{pump} + X_g} \quad (29)$$

$$\eta_3 = \frac{exergy\ output}{total\ exergy\ input} = \frac{X_{out}}{E_{comp} + E_{CP} + E_{pump} + X_g} \quad (30)$$

Sensitivity Analysis

The influence of varying temperature conditions on the exergy performance of the individual system components is assessed by varying each boundary temperatures separately, while keeping the remaining temperatures at their base values. The reference temperature T_0, ground temperature T_g, and indoor temperature T_{in} are varied according to their ranges given in Table 1, which refer to the typical range of conditions at the building location in Cambridge, UK.

In addition, we also analyse the effect of varying the difference between the ground temperature and the BHE outlet temperature dT_{gw}, the difference between the ceiling supply and indoor temperature dT_{ceil}, and the difference between the supply and the return temperature of the ceiling dT_{sup} (Table 1). The base values of these differences and the corresponding absolute temperatures reflect the design values of the system obtained from the technical documentation. The ranges of the individual temperature differences are chosen to reflect an approx. ± 50% change in exchanged energy amount across the corresponding component, which seems a physically reasonable range and will allow us to observe a distinct response based on the induced effect.

Table 1: System and boundary temperatures and the ranges used for sensitivity analysis.

boundary temperatures	**abbreviation**	**base value in K (°C)**	**minimum value in K (°C)**	**maximum value in K (°C)**
reference temperature	T_0	303 (30)	298 (25)	308 (35)
ground temperature	T_g	286 (13)	283 (10)	288 (15)
indoor temperature	T_{in}	294 (21)	293 (20)	297 (24)
temperature adaption in the BHE T_g-T_{gw}	dT_{gw}	4	2	6
BHE outlet temperature	$T_w = T_g + dT_{gw}$	290 (17)	285 (12)	294 (21)
ceiling temperature spread	dT_{ceil}	4	2	6
ceiling supply temperature	$T_{sup} = T_{in} - dT_{ceil}$	290 (17)	287 (14)	295 (22)
supply temperature spread T_{sup}-T_{re}	dT_{sup}	3	1	5
ceiling return temperature	$T_{re} = T_{sup} + dT_{sup}$	293 (20)	288 (15)	300 (27)
condensing temperature	$T_c = T_w + 10$	300 (27)	295 (22)	304 (31)
evaporation temperature	$T_e = T_{re} - 8$	285 (12)	280 (7)	292 (19)
HP load inlet temperature	$T_{HP,in} = T_{re}$	i.e. no heat loss or gain between ceiling outlet and heat pump inlet		
HP mixing valve temperature	$T_{mix} = T_{sup}$	i.e. no heat loss or gain between HP mixing valve and ceiling inlet		
HP load return temperature	$T_{HP,out}$	set to meet energy balance in mixing valve		
BHE inlet temperature	$T_{w,re}$	set to meet energy balance in heat pump		

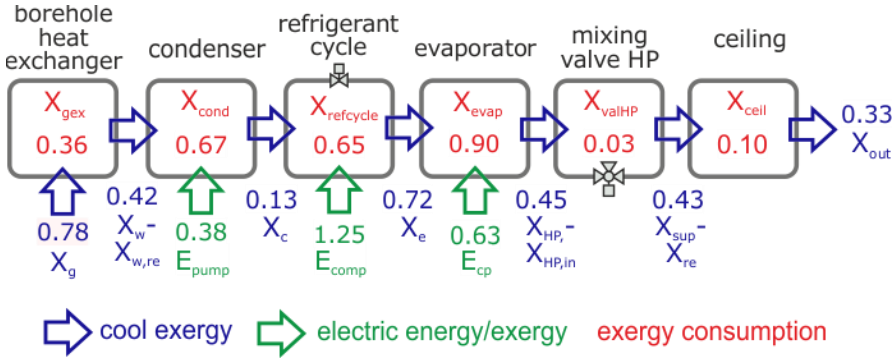

Figure 3: Exergy values in kW for the individual system components in cooling mode. Blue arrows indicate cool exergy flows, green arrows electricity input to the system and exergy consumptions are labelled in red.

T_c, T_e, and their ranges are set to match the inlet and outlet temperatures on either side of the heat pump as specified in the technical documentation of the system, and fall within the range of typical values (Li et al., 2014; Bi et al., 2009). All remaining temperatures that have to be specified for the exergy analysis depend either on these temperatures and temperature differences, or are inferred during the analysis given the current state of the system and the principle of energy conservation.

To determine the magnitude of the impact of varying temperature parameters on the overall system exergy performance and to identify the most influential temperature parameter, we perform a sensitivity analysis using Morris method, which is often applied to building or energy supply models (Morris, 1991). Morris method is based on a factorial sampling strategy, where the parameters space is transferred into a multidimensional hypercube with a unit length. The sampling process starts at a random grid point of the hypercube and for each new sample there is a unit change in exactly one dimension so that only one parameter value changes at the time. After creating several such sample sequences, the corresponding model results are evaluated with regard to the median value of the results to evaluate the impact of each parameter on the model outcome (Menberg et al, 2016).

Exergy Analysis of GSHP system

Figure 3 shows the results for the exergy input, flow and consumption values of each component in the system using base values listed in Table 1. The detailed analysis of the individual components allows an assessment of the performance of the individual subsystems. The exergy values for the ground heat exchanger indicate that almost 50% of the exergy extracted from the ground (X_g) are consumed during heat exchanges (X_{gex}) so that 0.42 kW are transferred to the condenser. X_{gex} accounts for irreversible thermodynamic effects during exergy transfer between exergy carriers, such as the ground and the heat carrier in the BHE, and friction between the fluids and pipework.

With temperature differences between T_0, T_{re}, T_{sup} and T_{in} being relatively small, only a quarter of the exergy transferred into the ceiling is consumed, while exergy consumption in the heat pump is relatively large due to the larger differences between T_w, T_c, T_e and T_{re}.

Components with a lower temperature spread between inputs and outputs, such as the mixing valve, show a very low exergy consumption and thus favourable ratios of exergy input to exergy output. The exergy input by the electric components (such as the pumps) represent a necessary input to the system to drive the fluid that transports the exergy through the system to its output location.

The net exergy efficiency of the system is η_1 is 14.6%, while the natural exergy efficiency accounts up to 25.6%, which indicates that over a quarter of the system exergy input comes from the natural, sustainable resource. The true exergy efficiency is 10.9% showing that the largest portion of the exergy input is consumed within the system.

Parametric variation of temperature conditions

In the following sections, the results for the parametric variations for each temperature are shown and discussed for the individual components. The values for the mixing valve of the heat pump are not included because of the minor exergy consumption in this component. While the absolute values of the different exergy parameters apply only to the investigated system and the chosen system settings, the observed trends in exergy values with varying temperatures and relations between individual components are transferable to other GSHP systems and different temperature conditions.

Reference temperature

As expected based on the relation in eq. 4a, exergy input, output and consumption values of all components are significantly affected by changes in the reference temperatures, within the 10 K range specified in Table 1. Figure 4 shows the influence on borehole heat exchanger component: the increase in the reference temperature leads to a considerably increasing exergy input ($X_{w,re}$) and output (X_w), while the exergy consumption (X_{gex}) exhibits only a very slight increase (Figure 4).

The exergy content of the BHE outlet flow X_w tends towards zero as the reference temperature drops and the temperature difference between T_0 and T_w becomes smaller. Recalling the definition of exergy, the dispersion potential of the system becomes zero, when the system is in thermal equilibrium with its reference state.

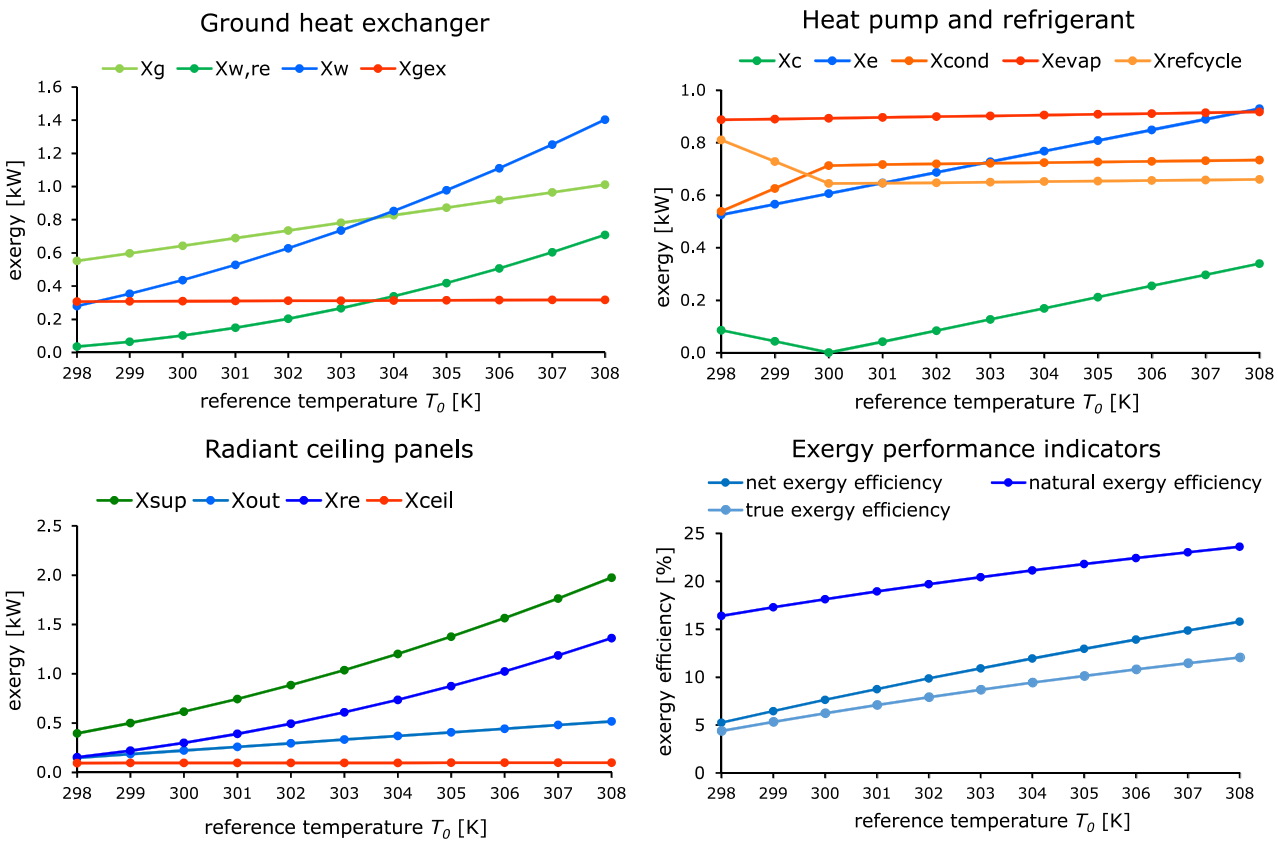

Figure 4: Exergy values in the borehole heat exchanger, heat pump and refrigerant, and radiant ceiling component and exergy performance indicators for a varying reference temperature T_0.

This effect can also be observed in the heat pump component and the refrigerant (Figure 4). Again, the changes in reference temperature have a more significant effect on the exergy input (X_e) and output (X_c,) than on the exergy consumption (X_{evap}, X_{cond}, $X_{refcycle}$) where the effect is scarcely visible. With the condensing temperature being set to 300K, the dispersion potential and exergy output (X_c,) at a reference temperature of 300K are zero. When the reference temperature becomes lower than 300K, the dispersion potential increases again. However, in this case T_0 is smaller than the system temperature T_c so that the exergy is comprised of warm exergy (eq. 1), which results also in a change of the exergy flow direction and significant changes in the corresponding exergy consumption terms (X_{cond}, X_{evap}).

For the radiant ceiling, the observed effects are very similar to those in the previous components. As shown in Figure 4, exergy input (X_{sup}) and output (X_{re}, X_{out}) values show a significant increase with an increasing reference temperature, and tend towards zero as T_0 becomes similar to the indoor temperature T_{in}. Variation in the exergy consumption in the ceiling (X_{ceil}) is again comparably small.

In accordance with the variation in exergy inputs and outputs for the individual components, the overall system exergy input and output show a significant increase with increasing reference temperature. The exergy consumption on the other hand is less sensitive to an increase in T_0, as it mainly depends on the temperature spread across the components. These changes lead then to a considerable increase in the exergy performance indicators with T_0 (Figure 4) indicating that the cooling supply system performs more efficiently, when outdoor temperatures are warmer. This effect is more dominant for the net exergy efficiency η_1 because this indicator does not depend on the varying X_g.

Ground temperature

As one would expect, the variation of the ground temperature has a significant effect on the exergy values related to the BHE component (Figure 5, top). As we are investigating the GSHP's potential to provide cooling, the cool exergy values drop with increasing ground temperature. This effect is again more prominent for exergy input ($X_{w,re}$) and output (X_w) values than for exergy consumption (X_{gex}).

Regarding the magnitude of the changes in exergy values per 1 K change in the boundary temperature, the impact of T_0 and T_g on the exergy values in the BHE is almost identical. Looking at the exergy values in the heat pump and refrigerant cycle reveals that changes in T_g only affect the source side values at the condenser (X_c, X_{cond}) and the exergy consumptions in the refrigerant ($X_{refcycle}$), which depends on the difference between T_w and T_{re} (Figure 5, middle).

This is because the temperature difference between BHE inlet and outlet remains constant (Table 1), and consequently the amount of energy extracted from the ground

does not increase with T_g, as one might expect. Consequently, varying thermal ground conditions have also no effect on the amount of energy transferred through the heat pump or the room. However, the negative influence of T_g on X_g results in a decrease of the natural exergy efficiency indicating that the relative amount of natural exergy available for cooling decreases with higher ground temperatures (Figure 5, bottom). The opposite changes for η_1 and η_3 results from the decrease in $X_{refcycle}$.

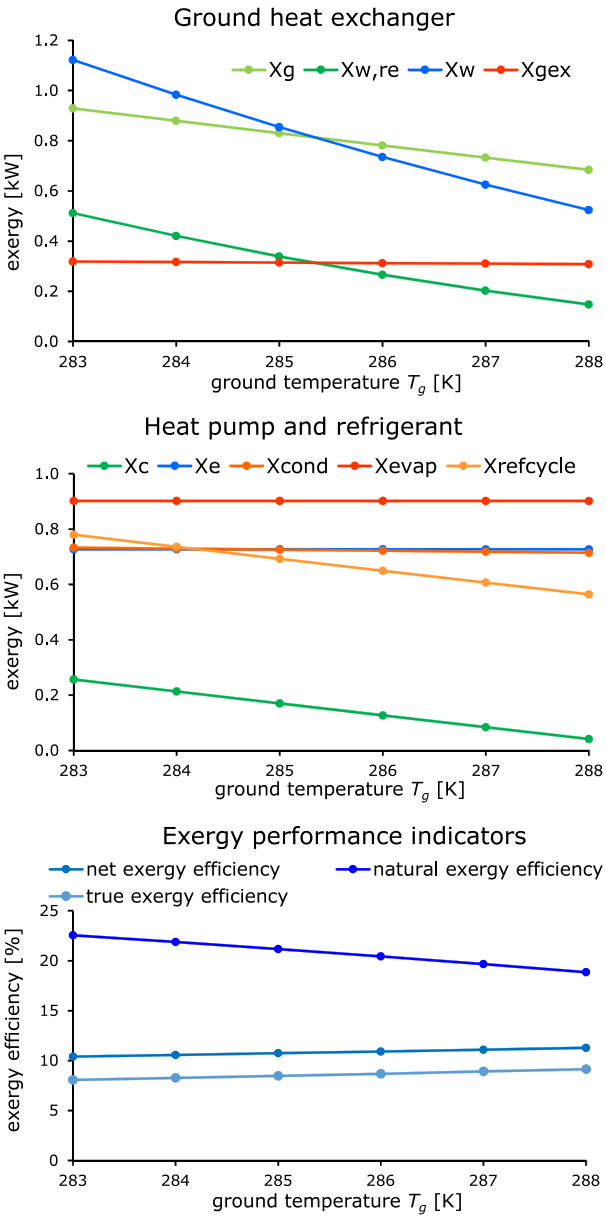

Figure 5: Exergy values in the borehole heat exchanger and heat pump/refrigerant component, and exergy performance indicators for a varying ground temperature T_g.

Indoor temperature

Changes in indoor temperature have no effect on any exergy values in the BHE and on the source side of the heat pump, because they do not influence the amount of exchanged energy or the temperatures in these components. Significant changes with T_{in} are observed for X_e and $X_{refcycle}$, which are linked to the increase in T_{re} with higher T_{in} (Table 1), and in the radiant ceiling (Figure 6, top and middle). While the amount of cool energy delivered to the indoor space is constant, the exergy values for the radiant ceiling fall significantly for increasing T_{in}, because the dispersion potential decreases as T_{in} increases towards T_0. This results in lower net and true exergy efficiencies for higher T_{in}, while the natural exergy efficiency is unaffected (Figure 6, bottom). For system operation strategies, this means that increasing the cooling set point temperature (without decreasing the actual cooling demand) leads to a significant decline in cooling efficiency.

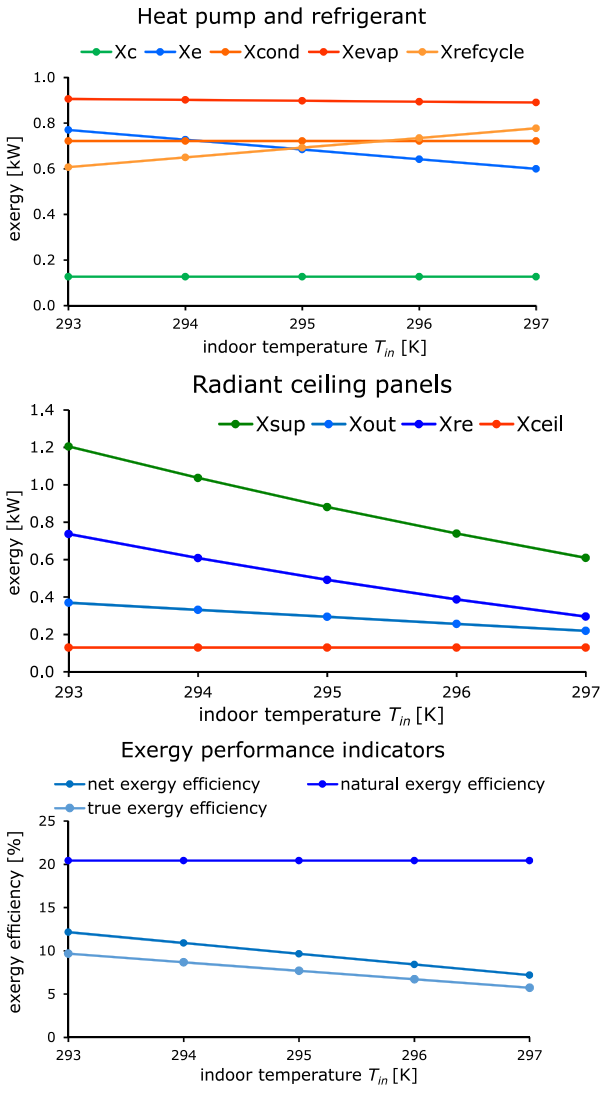

Figure 6: Exergy values in the heat pump/refrigerant and in the radiant ceiling component, and exergy performance indicators for a varying indoor temperature T_{in}.

Temperature adaption in the BHE dT_{gw}

In this section, we evaluate the influence of the magnitude of temperature adaption in the BHE, i.e. the temperature difference between T_g and the heat carrier temperature T_w, which ultimately determines the value of T_w. Figure 7

shows the resulting decrease in exergy contents in the heat carrier, X_w and X_{wre}, which is linked to the reduction in dispersion potential with higher fluid temperatures. A larger temperature spread across the BHE leads to higher exergy consumption (X_{gex}), which is cancelled out by a decrease in $X_{refcycle}$, as the temperature spread across the heat pump inlet flows (T_{HPin} - T_w) becomes smaller.
Due to the unchanged overall exergy input and output, dT_{gw} has no impact on the overall exergy performance on the system. The absolute temperatures in the heat carrier fluid in the BHE are consequently of no importance for the cooling efficiency of the system, as long as the temperatures differences and energy transfer rates are constant.

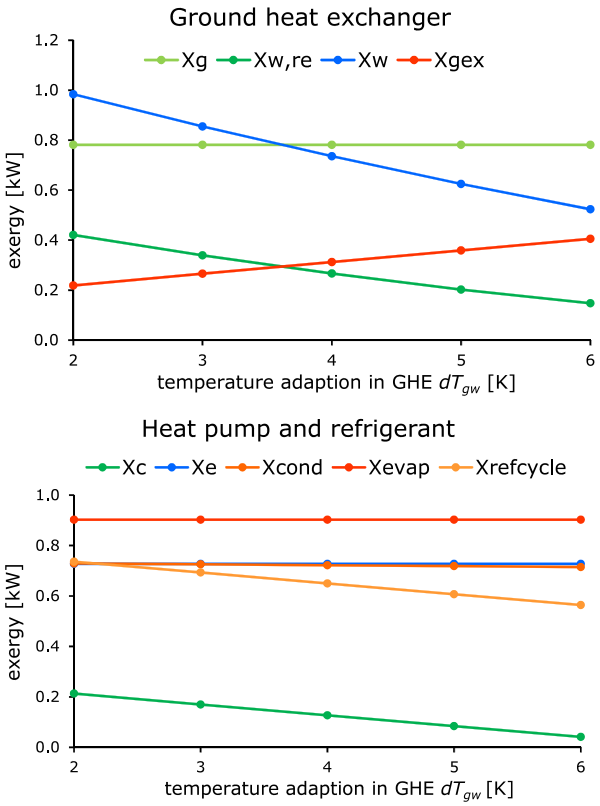

Figure 7: Exergy values in the borehole heat exchanger and the heat pump/refrigerant component for a varying temperature adaption in the BHE dT_{gw}.

Ceiling temperature spread dT_{ceil}

Changes in the temperature spread dT_{ceil} between T_{sup} and T_{in} influence the same system components as variation of T_{in}, but in the opposite direction (Figure 8). Lower values for T_{sup}, and consequently T_{re}, results in larger exergy inputs from the HP load side, X_e, and less consumption in the HP due to a lower temperature difference between T_{HPin} and T_w. On the other hand, the larger difference between T_{sup} and T_{in}, causes an increase in the exergy consumption in the ceiling, X_{ceil}, which cancels out the positive effect in the heat pump. Similar to dT_{gw}, the temperature spread across the ceiling dT_{ceil}, has no influence on the overall system performance and does consequently not need to be considered for improvement measures for system efficiency.

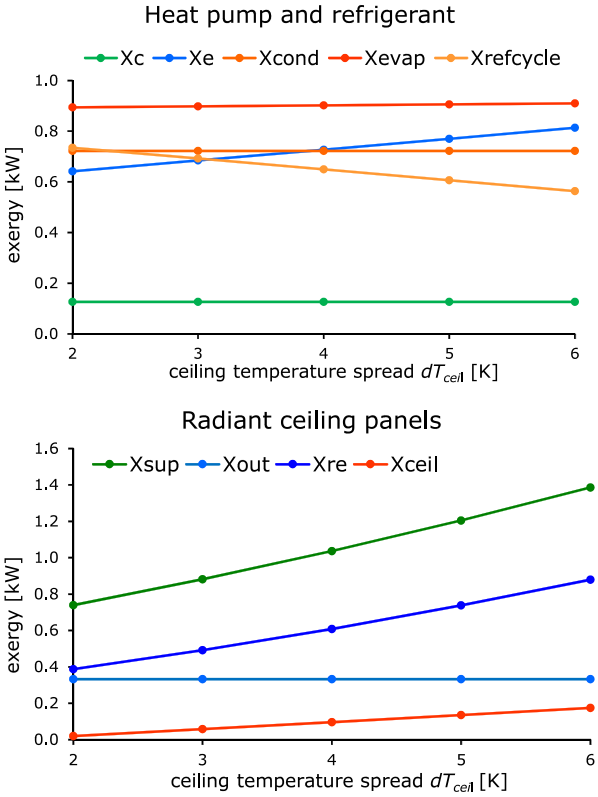

Figure 8: Exergy values in the heat pump/refrigerant and in the radiant ceiling component for a varying ceiling temperature spread dT_{ceil}

Supply temperature spread dT_{sup}

Contrary to the previously regarded temperature spreads, the difference between T_{sup} and T_{re}, dT_{sup}, has a significant influence on all components (Figure 9). It determines the amount of energy exchanged through the radiant ceiling Q_{out}, and consequently Q_g, Q_c, Q_e, and all related exergy values. At the same time, an increase in dT_{sup} causes an increase in T_{re} (Table 1), which adds further changes in the exergy values, and causes non-linear trends in the BHE and heat pump components. This effect is very significant for the exergy consumption in these components, which is very sensitive to larger energy exchanger and higher temperature differences (Figure 9, top). Some of the changes in exergy consumption counteract, but there is still a significant effect on the overall system performance.
All three exergy efficiency indicators show a significant increase with increasing dT_{sup}, which is caused by a considerable increase in the exergy output (Figure 9, bottom left). These graphs suggest good opportunities for system improvement with regard to dT_{sup}, although the decline in increase for higher dT_{sup} suggest a limit for efficiency improvement.

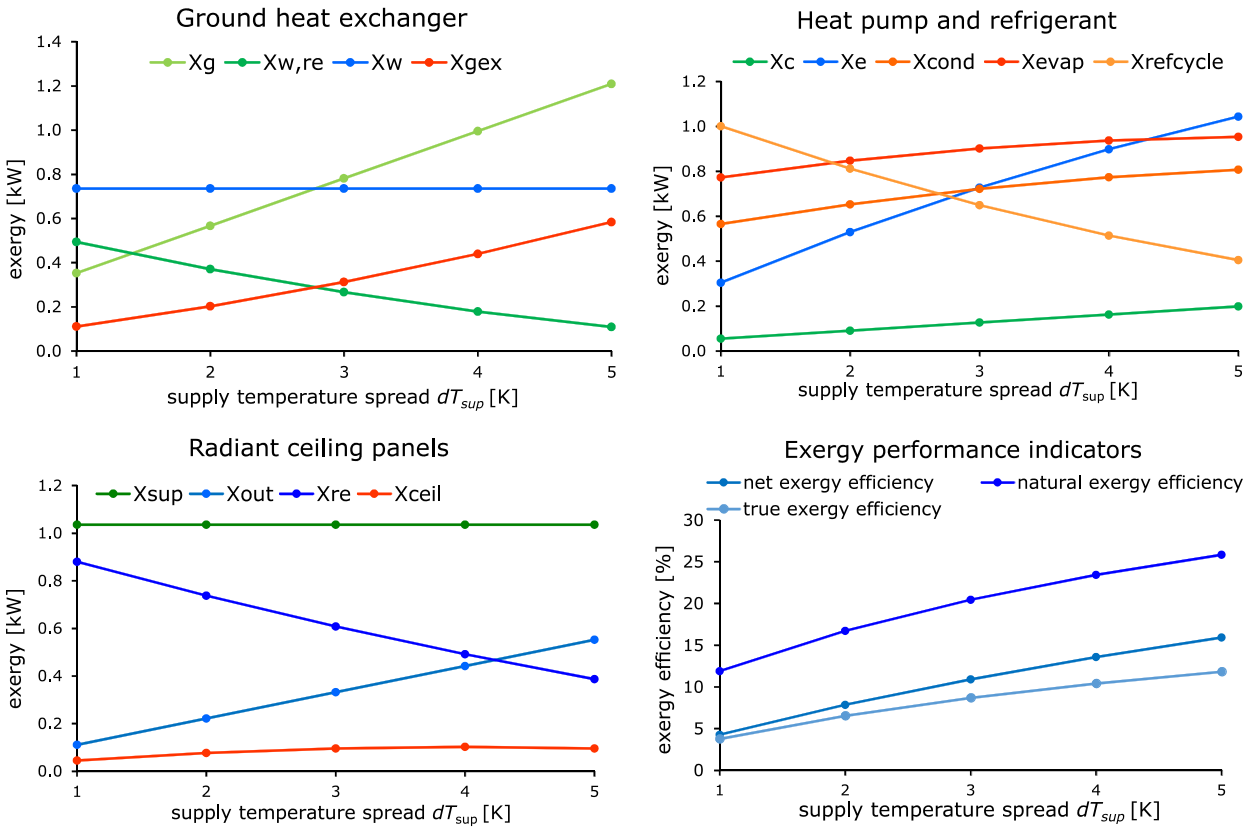

Figure 9: Exergy values in the borehole heat exchanger, heat pump/refrigerant, and radiant ceiling component and exergy performance indicators for a varying supply temperature spread dT_{sup}.

Sensitivity analysis with Morris method

The results from the sensitivity analysis with Morris method are displayed in Table 2 and show the overall magnitude of influence of the selected boundary temperatures and temperature spreads on the three investigated exergy efficiency indicators. For the interpretation of Morris method results, it is important to distinguish between negligible parameters that have only a very small, but noticeable, impact on the model outcome and parameters that exhibit exact zero values and have absolutely no effect on the model results.

The values in Table 2 reveal that of the three examined temperature boundaries, the reference temperature T_0 has the largest impact on all three performance indicators. T_g has a significant impact on the natural exergy efficiency, but only a minor impact on the net and true exergy efficiency, which can be explained by the rather large amount of exergy input through the electric equipment compared to the amount of exergy from the ground. The indoor temperature has no effect on the natural exergy efficiency, as observed for variation of T_{in} above, and significantly less impact on the other two indicators than T_0.

Regarding the impact of the investigated temperature spreads across different system parts, the supply temperature spread dT_{sup} has clearly the most significant impact, which is in the same order of magnitude as the effect of T_0. dT_{gw} and dT_{ceil} only influence those performance indicators that relate to the components they affect (see discussion above), and only to a negligible amount, because their effects often cancel out through other components.

Table 2: Results for sensitivity analysis with Morris method as median values of the elementary effects in kW for the investigated temperature parameters and exergy performance indicators.

Performance indicators	T_0	T_g	T_{in}	dT_{gw}	dT_{ceil}	dT_{sup}
Net exergy efficiency	11.39	1.36	6.43	0	9×10^{-15}	8.60
Natural exergy efficiency	7.01	4.39	0	5×10^{-15}	0	12.27
True exergy efficiency	8.42	1.53	4.97	0	5×10^{-15}	5.71

Conclusion

Examination of a detailed thermodynamic model of a GSHP cooling system with the concept of warm and cool exergy enables an in-depth assessment of the utility of individual system components, such as the borehole heat exchanger (BHE), the heat pump, and the radiant ceiling. This study reveals that the exergy consumption in these components is closely related to the temperature spread across the individual subsystems. For example, subsystems with a smaller temperature difference between source and load side, such as the BHE and radiant ceiling, have lower exergy consumption than the components of the heat pump.

Parametric variation of fluid temperatures, by varying parameters such as the adaption of the heat carrier fluid in the BHE dT_{gw}, results in significant changes in exergy values within the individual components and reveals diverse interactions between components. In particular, the differences in exergy consumption terms resulting from temperature changes often counteract each other so that the overall system performance remains constant over the investigated temperature ranges. As shown in Figures 7 and 8, this effect is primarily observed for changes in absolute fluid temperatures that only influence the exergy values in certain components, where the changes in exergy consumption then cancel out.

Changes in system temperatures, such as the ground temperature T_g, on the other hand are found to influence the overall system performance, as they cause changes in the amount of energy exchanged between components, or alter the temperature spread across the entire system, i.e. from the ground to the indoor space (see Figure 9). Hence, the boundary temperatures of the cooling system, T_g and T_{in}, play an important role for the system efficiency and should be considered carefully for system design, evaluation and operation.

The reference temperature, T_0, has the by far largest impact on the system efficiency, which is not surprising given its dominant role in the governing equations. Thus, the type and value of the temperature used as reference condition should be carefully considered. The temperature difference dT_{sup}, which determines the energy output, is found to be almost as influential as T_0, and consequently offers opportunities for potential system improvement.

In addition, we find that varying temperatures, such as the reference or ground temperature, across wide ranges require special attention to the temperature relations within the subsystems, as they determine the type of exergy (warm or cool) and the flow direction of exergy. These results demonstrate how exergy analysis, in contrast to energy analysis, enables a better assessment of the utility within each individual component of an energy system. As such, it offers a powerful framework through which one can identify critical parameters influencing system (in)efficiencies across its components. Thus, incorporating exergy models into existing energy simulation tools appears to be a promising option to further enhance in-depth system performance analysis. However, further work is needed to adapt our steady-state model in order to enable coupling to transient system or building simulations.

Acknowledgements

This study is supported by EPSRC grant (EP/L024452/1): Bayesian Building Energy Management (B-bem).

References

Kazanci, O.B., Shukuya, M. and B.W. Olesen (2016). Theoretical analysis of the performance of different cooling strategier with the concept of cool exergy. *Building and Environment 100*, 102-113.

Menberg, K., Heo, Y. and R. Choudhary (2016). Sensitivity analysis methods for building energy models: Comparing computational costs and extractable information, *Energy and Buildings 133*, 433-445.

Morris, M. D. (1991). Factorial sampling plans for preliminary computational experiments. *Technometrics 33*, 161-174.

Li, R., Ooka, R. and M. Shukuya (2014). Theoretical analysis on ground source heat pump and air source heat pump systems by the concepts of cool and warm exergy, *Energy and Buildings 75*, 447-455.

Schmidt, D. (2009). Low exergy systems for high-performance buildings and communities, *Energy and Buildings 41*, 331-336.

Shukuya, M. (2013). Exergy: theory and applications in the built environment. *Springer*, 364 p.

Bi, Y., Wang, X., Liu, Y., Zhang, H. and L. Chen (2009). Comprehensive exergy analysis of a ground-source heat pump system for both building heating and cooling modes. *Applied Energy 86*, 2560-2565.

Zhou, Y. and G. Gong (2013). Exergy analysis of the building heating and cooling system from the power plant to the building envelop with hourly variable reference state. *Energy and Buildings 56*, 94-99.